Conference paper

Ashim Nandi, Adam Sucher, Anat Tyomkin and Sebastian Kozuch*

Ping-pong tunneling reactions, part 2: boron and carbon bell-clapper rearrangement

https://doi.org/10.1515/pac-2019-0401

Abstract: Anthracene can be used as a scaffold for intramolecular S_N^2 degenerate reactions of the "bell clapper" type, where a central boron atom or its isoelectronic carbocation bonds alternatively towards one or the other lateral Lewis bases at the first and eight anthracene positions. This ping-pong bond-switching reaction possesses a symmetrical double-well potential with low activation barrier and relatively narrow barrier width. Herein we show by computational means the active role played by heavy atom quantum tunneling in this degenerate rearrangement reaction at cryogenic temperatures. At these conditions the thermal "over the barrier" reaction is forbidden, whereas the tunneling effect enhances the rate of reaction up to an experimentally measurable half-life. Kinetic isotope effects and cryogenic NMR spectroscopy can, in principle, experimentally demonstrate the tunneling mechanism.

Keywords: bell-clapper reaction; boron; computational chemistry; ICPOC-24; kinetic isotope effect; kinetics; NMR; quantum tunneling.

Introduction

A good deal of attention has been paid to the established chemistry of hypercoordinated compounds [1–6] (also called, controversially, hypervalent systems) by both experimentalists and theoreticians, due to their unique reactivity and properties. These molecules are usually described by a three-center four-electron bond [6, 7], and are typical within main group elements in and below the third row of the periodic table. Pentacoordinated bond formation by second row elements such as carbon and boron are, due to their low polarizability and high relative electronegativity, very scarce (though the trigonal bipyramidal geometry is common in the transition state of S_N^2 reactions). Still, they are possible, as many computational and experimental studies have shown [4, 8–18]. For example, Akiba et al. [19, 20] used an anthracene scaffold to synthesize potentially pentacoordinated carbocation and boron containing compounds (see $C_{R,Y}$ and $B_{R,Y}$ in Fig. 1). Although some species have very loose bonding between the boron or the carbocation to the lateral Lewis bases, and therefore cannot be considered as hypercoordinative (for instance $B_{OMe,OMe}$), other molecules have tight symmetrical binding, showing a clear symmetrical pentacoordinated geometry (such as B_{FOMe}) [20].

Yet, other species prefer an unsymmetrical geometry, with the central atom leaning to one or the other donor group (for example $B_{Me,NMe2}$ or $B_{Cl,NMe2}$) [20]. These almost symmetrical molecules are of particular interest for the present research, as they can undergo a very fast intramolecular degenerate bond-making and breaking between the sp³ central atom and the lateral substituents. This rearrangement occur through a

Article note: A collection of invited papers based on presentations at the 24th IUPAC International Conference on Physical Organic Chemistry (ICPOC 24) held in Faro, Portugal, 1–6 July 2018.

Ashim Nandi, Adam Sucher and Anat Tyomkin: Department of Chemistry, Ben-Gurion University of the Negev, Beer-Sheva 841051, Israel

© 2019 IUPAC & De Gruyter. This work is licensed under a Creative Commons Attribution-NonCommercial-NoDerivatives 4.0 International License. For more information, please visit: http://creativecommons.org/licenses/by-nc-nd/4.0/

^{*}Corresponding author: Sebastian Kozuch, Department of Chemistry, Ben-Gurion University of the Negev, Beer-Sheva 841051, Israel, e-mail: kozuch@bgu.ac.il. https://orcid.org/0000-0003-3070-8141

symmetrical S_N^2 mechanism, as was shown by ¹H NMR and DFT studies, in what was called a "bell-clapper" mechanism (Fig. 1) [3, 21, 22]. The energy barrier for this rearrangement reaction was found to be too small to measure by the NMR coalescence method. Encouraged by the low barrier and small displacement of the central carbon or boron, we envisaged that these reactions may occur by heavy atom tunneling, analogous to a quantum ping-pong game [23].

Quantum mechanical tunneling (**QMT**) of hydrogen is a well-known effect that has been widely studied both experimentally and theoretically [24, 25]. The extent to which tunneling occurs in a chemical reaction depends on the barrier width (w), barrier height (ΔE^{\dagger}), and atomic masses (m) of the moving parts of the molecule, according to:

$$P \approx e^{-xw\sqrt{\Delta E^* m}} \tag{1}$$

where *P* is the tunneling probability ("barrier permeability"), and *x* is a factor that depends on the shape of the potential energy curve [24]. It can be seen from eq. 1 that the tunneling probability is particularly sensitive to the barrier width (a variable with no significance in semi-classical transition state theory), making the amplitude of the atomic movements the most critical factor for a swift tunneling. In this sense, it was recently shown that "heavy" atom tunneling (i.e. atoms from the second row of the periodic table) is indeed possible, as long as the barrier height is low and, more important, the barrier width is markedly narrow [24, 26]. The first experimental evidence of such kind of tunneling was found in the automerization (aka π -bond shifting) of cyclobutadiene [27–29]. From there, several other documented reactions emerged, such as the ring expansion of methyl-cyclobutyl-fluorocarbene [30], ring opening of cyclopropyl-carbinyl radical [31, 32], degenerate rearrangement of semibullvalene [33, 34], ketenimine ring expansion [35], and ring closure of cyclopentane-1,3-diyl [36, 37] (see also Refs. [26, 38, 39] and references within). All these examples share the already cited characteristics: a low and narrow activation barrier. To the best of our knowledge, the heaviest atom predicted to tunnel from the ground state in a realistic (albeit theoretical) reaction involves a fluorine, in another case of a quantum ping-pong mechanism [23]. We can divide all these reactions in two groups, the exothermic ones (asymmetric reaction profiles such as the cited ring expansion, opening or closing), and the isothermic ones (degenerate rearrangements with symmetric reaction coordinates, such as the cyclobutadiene and semibullvalene cases). In the latter group, which includes our current bell-clapper reaction, we can also find many examples of H-transfer, such as proton sponges and formic acid dimer [40-42].

In this work, through computational tools we predict the boron and carbon atom tunneling by rapid bond switching on the bell clapper mechanism (Fig. 1). Additionally, we propose an experimental test to check the QMT effect by NMR spectroscopy.

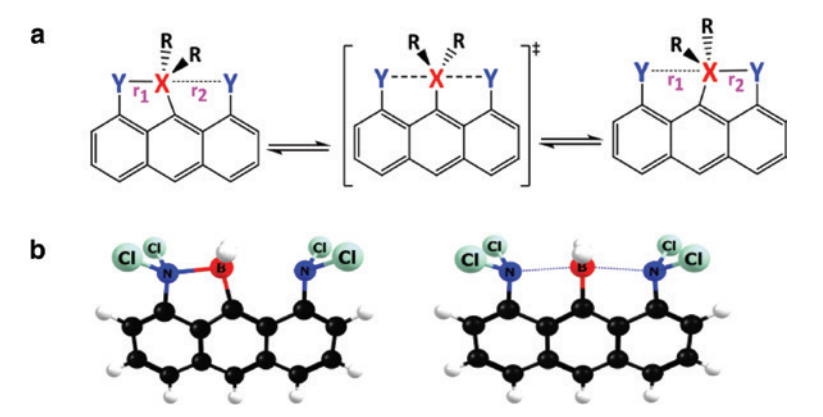


Fig. 1: (a) Bell-clapper degenerate reactions for $\mathbf{B}_{\mathbf{R},\mathbf{Y}}$ and $\mathbf{C}_{\mathbf{R},\mathbf{Y}}$ (X = B or C⁺). In many cases the symmetrical structure is sufficiently stabilized to produce a single pentacoordinated species instead of the degenerate double-well system. (b) Optimized structures of $\mathbf{B}_{\mathbf{H},\mathbf{NCI2}}$ at \mathbf{C}_{s} (stable geometry) and \mathbf{C}_{2v} (transition state) symmetry.

Theoretical method

To accurately account for the rates of reaction, especially including tunneling corrections, it is critical to properly describe the potential energy surface. Hence, in order to select a suitable functional and basis set in terms of accuracy and computational cost, we performed benchmark calculations on the barrier height (ΔE^{\dagger}) of the title reaction using fourteen different DFT functionals (four GGAs –B97D3, PBE, BLYP and BP86–, three meta-GGAs -BB95, MN15L and TPSS-, three hybrid-GGAs -PBE0, TPPSh and B3LYP-, and four hybridmeta-GGAs –B1B95, BMK, MN15 and M06-2X–) in combination with five basis sets (Def2-SVP, 6-31+G(d), 6-31+G(d,p), aug-cc-pVDZ and aug-cc-pVTZ, the latter taken only as a reference, as it is currently impossible to carry out SCT tunneling computations on medium sized molecules with this basis set). All these methods were benchmarked against DLPNO-CCSD(T)/aug-cc-pVQZ//MN15/aug-cc-pVTZ energies for the rearrangement of $\mathbf{B}_{H \text{ NF2}}$ and $\mathbf{C}_{H \text{ NH2}}$. The resulting best combination (ΔE^{\dagger} within 0.9 kJ·mol¹ for the former and 0.5 kJ·mol⁻¹ for the latter), and the one we used for all the computations, was MN15/aug-cc-pVDZ [43], a method that stretched our computation capabilities to the limit. DFT geometry optimizations and frequency calculations were carried out with Gaussian16 [44], while the DLPNO-CCSD(T) [45, 46] benchmark was computed with ORCA4.0 [47, 48] with the "tightPNO" option [48].

For the tunneling corrections there are various approximate methods that can be used to study the reaction rate, such as the use of a parabolic potential, the Eckart barrier, or the renowned Wigner approximation [24]. However, these approximations lack the thermal-activated tunneling correction from the vibrationally excited states level and the possibility to "cut-corners" to pass through the least-action pathway (were the barrier height may be higher than the TS, but the atom trajectory, the main factor for a fast QMT, is shorter) [49]. A highly demanding but accurate method that include the above effects is the small-curvature tunneling (SCT) methodology [49, 50]. This method has the extra capability of mapping the potential energy surface with multidimensional contributions by calculating energies, gradients and second derivatives not only at the reactant and transition state geometries, but also at many points along the reaction pathway. We carried out all the semi-classical dynamics with the canonical variational transition-state theory (CVT) [51], and the QMT corrections with SCT using the POLYRATE package [52], with GAUSSRATE [53] as the interface with Gaussian 16. After some accuracy tests we decided to use a step size of 0.002 Bohr, with the quantized reactant state tunneling (QRST) method [54].

As a crude but fast method to pre-filter the systems with potential for reacting via QMT at cryogenic temperatures, we considered the tunneling limit (T_i) approximation [23, 55]. This expression, based on eq. 1, is written as:

$$T_{L} = \frac{W_{1/2} \sqrt{\Delta E^{*}m}}{\hbar} \tag{2}$$

where m is the mass of the tunneling determining atom (**TDA**) whenever there is a clear one (see below), ΔE^{\dagger} the activation energy, and $w_{1,2}$ the barrier width taken at half the barrier height (in here we estimated it by the difference between the long and short X–Y distances divided by two). Previous tests indicate that T_t linearly correlates with the logarithm of accurately computed rates [23, 55], where reactions with T_i < 10 could, in principle, react by QMT from the ground state in a sensible experimental time.

Results and discussion

Figure 1 shows the key intramolecular S_N^2 reaction (bell-clapper mechanism) for $\mathbf{B}_{R,Y}$ and $\mathbf{C}_{R,Y}$. This reaction undergoes a bond switching between the central X and lateral Y groups via a C₂ trigonal bipyramidal transition state structure which resembles a pentacoordinated bonding pattern, with a symmetrical double-well potential energy surface. Table 1 lists the activation energy, the bond length of the bonded (r_.)

Table 1: Activation energy (ΔE^{\pm} in kJ·mol ⁻¹), short and long bond lengths (r_1 and r_2 in Å), effective barrier width ($w_{i,j}$ in Å) and
dimensionless tunneling limit (T_i) .

	Δ <i>E</i> ‡	r _i	r ₂	W _{1/2}	T _L
B _{Cl,NMe2}	39.7	1.675	3.137	0.73	24.4
B _{H,NH2}	68.2	1.665	2.975	0.66	28.9
B _{H,NMe2}	35.5	1.683	2.970	0.64	20.4
B _{H,NF2}	21.3	1.714	2.858	0.57	14.0
B _{H,NCl2}	8.8	1.801	2.742	0.47	7.4
B _{H,NBr2}	9.6	1.791	2.736	0.47	7.7
C _{H,NH2}	78.6	1.548	2.860	0.66	32.2
C _{H,Cl}	18.6	1.912	2.865	0.48	11.5
C _{H,Br}	20.0	2.036	2.974	0.47	11.7

and non-bonded (r_j) X–Y bond, the effective barrier width $(w_{i,j})$ and the tunneling limit (T_j) for $\mathbf{B_{RY}}$ and $\mathbf{C_{RY}}$ studied systems.

In the original **B**_{CLNMe2} system reported by Akiba et al. our computed activation energy is 39.7 kJ·mol⁻¹, with bond distances of 1.675 and 3.137 Å for the shorter (r₁) and longer (r₂) B–N distances (see Table 1 and Fig. 1), in good agreement with the X-ray diffraction analysis ($r_1 = 1.664$ and $r_2 = 3.129$ Å) [20]. The effective barrier width $(w_{1/2} = 0.73 \text{ Å})$ is significantly narrower than the complete movement that the boron must travel, but it is a more accurate proxy to use for the T_i ; close to the minima the displacement of the atom requires a negligible energy, and therefore those sections of the reaction coordinate are kinetically irrelevant for tunneling. Still, the high T_L value of 24.4 for \mathbf{B}_{CLNMe2} indicates that the reaction will not occur by QMT from the ground state. We therefore tuned the system by attempting various substitutions that would shrink both the barrier height and width, thus giving better candidates for tunneling. Due to clashing effects, this process is more trial an error than a systematic search. For instance, a weaker Y electron donor will make the short X-Y bond (r,) more labile and longer (with a lower ΔE^{\dagger}), but it will make the long X–Y bond (r₂) longer as well, compensating the effect; therefore, a weaker Y nucleophile may or may not lower $w_{i,j}$ and T_i . Similarly, a strong σ electron withdrawing atom in the R groups may also act as a π donor (as in the case of halogens), blurring the possibility of predictions. In addition, some steric hindrance pushes the Y groups inside (for instance when comparing Y=NH, and NMe,), changing the potential energy surface exclusively by brute force. Still, a couple of rules of thumb can be grasped: the asymmetric potential with higher activation energy tends to be favored by stronger Y electron donors (compare $\mathbf{B}_{H.NH2}$ to $\mathbf{B}_{H.NC2}$) or by weaker R π donors ($\mathbf{B}_{H.NF2}$ vs. $\mathbf{B}_{CL.NF2}$, the latter being a symmetrical pentacoordinated species, and therefore not included in Table 1). These effects strengthen the charge transfer interaction between X and Y.

Analyzing the trends between similar systems in Table 1 we can still find one clear, expected trend. Narrower $w_{i,j}$ correlates with lower ΔE^{\dagger} , hence both of them correlate with a smaller T_i . This can be explained by considering the harmonic potentials of the reactant and product states being closer, which puts the crossing point in a lower position [23]. Since our objective is to find systems with a fast QMT, low activation barriers should produce the desired outcome (as long as it is not so low that the system will prefer the C_w geometry!). Therefore, we carried out accurate QMT computations (SCT) on the most promising systems, $\mathbf{B}_{H \text{ NCP}}$ and $\mathbf{B}_{H \text{ NBP}}$. $(T_1 = 7.4 \text{ and } 7.7, \text{ respectively})$. To our delight, we obtained quite fast tunneling rate constants of 590 and 61 s⁻¹ $(t_{i,i}=1)$ and 11 ms), respectively, close to the absolute zero (that is, QMT from the ground state, where it is completely independent of the temperature). Considering that the computed semi-classical rates (CVT, without any tunneling correction) have the "impossible" values of $k = 5 \times 10^{-45}$ and 5×10^{-54} s⁻¹, we can ascertain that in cryogenic conditions the reaction occurs exclusively by a QMT mechanism. This might be, to the best of our knowledge, the first predicted case of a boron atom tunneling.

In parallel to the boron bell-clapper, also the isoelectronic carbocation-based reaction has been thoroughly studied in previous works [19-21], and therefore it is de rigueur to include it here. However, we must take into consideration that the necessary inclusion of a counterion in most experimental setup will change

the reaction [56], and therefore our computational results will only match the experiment where the carbocation can be isolated at low temperature (for instance in a supersonic expansion equipment). Due to the much stronger interactions with Y, carbocations have much higher activation energies, with very stable C. geometries. Hence, all the studied systems based on amine substituents were unsuitable for QMT ($T_c \gg 10$, see for example, $C_{H.NH2}$ in Table 1). However, with much weaker Y groups there is a slim chance, as can be seen in Table 1 for halides, with $T_L = 11.5$ and 11.7 for $C_{H,Cl}$ and $C_{H,Br}$, respectively ($C_{H,F}$ prefers the C_{2v} geometry). The ensuing SCT computations yielded $k = 7 \times 10^{-11}$ s⁻¹ when approaching the zero Kelvin regime for \mathbf{C}_{HBr} (with a semi-classical value of $k_{CVT} = 3 \times 10^{-139} \text{ s}^{-1}$ at 6 K), which can hardly be considered a realistic tunneling $(t_{1/2} = 300 \text{ years})$. But $\mathbf{C}_{H,Cl}$ gave $k = 6 \times 10^{-5} \text{ s}^{-1} (t_{1/2} = 3 \text{ h}, \text{ with } k_{CVT} = 7 \times 10^{-122} \text{ s}^{-1} \text{ at 6 K})$, well within what can be considered "experimental time". Therefore, this molecule can be included in the pantheon of systems that can react by carbon atom tunneling [26].

Figure 2a shows the Arrhenius plot of \mathbf{B}_{HNCD} and \mathbf{C}_{HCD} . In the low temperature region, the SCT rate constants deviates from the classical CVT rates reaching a clear plateau where the rates become independent of temperature, a distinct signature of tunneling from the ground state. For $\mathbf{B}_{\text{H-NCL}}$, at ~50 K the tunneling rate becomes dominant ($k_{\text{SCT}} = 4 \times 10^5 \text{ s}^{-1}$, $k_{\text{CVT}} = 9 \times 10^4 \text{ s}^{-1}$), while at ~30 K the semi-classical rate is negligible $(k_{SCT}=3\times10^3 \text{ s}^{-1}, k_{CVT}=3 \text{ s}^{-1})$. Below ~10 K the rate is entirely dominated by heavy atom tunneling from the ground state (note that in the case of hydrogen tunneling the vibrational states are usually more separated, showing larger independence from the temperature compared to heavy atom QMT). For $C_{H,CI}$ we start to see QMT dominance at ~75 K (k_{SCT} = 98 s⁻¹, k_{CVT} = 38 s⁻¹), negligible semi-classical reaction at ~40 K (k_{SCT} = 4×10⁻⁴ $\rm s^{-1}$, $k_{\rm CUT} = 10^{-8} \rm \ s^{-1}$), and exclusive tunneling from the ground state again at ~10 K.

Considering the fast tunneling rate of the $B_{H,NCl2}$ at cryogenic conditions, we decided to check the possibilities of QMT by substituting the lower carbon at the central anthracene ring. We expected that by having there a bulkier hetero atom, it will push out the lateral rings, bringing closer the Y groups and producing a narrower and lower rearrangement barrier. For this purpose we introduced a Si atom forming a 10-silaanthracene scaffold for $\mathbf{B}_{H,NCI2}$ (Scheme 1). Preliminary results suggested a large influence of the Si atom on the $w_{1/2}$ (0.41 Å) and ΔE^{\ddagger} (8.2 kJ·mol⁻¹), producing a T_{\bullet} of only 6.2. However, and to our surprise, the rate constant for this system was extremely slow ($k_{SCT} = 5 \times 10^{-07} \, \text{s}^{-1}$, with $t_{1/2} = 15 \, \text{days}$) at 6 K, which can barely be considered as a viable tunneling mechanism. This stark disparity between the accurate SCT rate constants and the T_i can be explained based on the displacement vectors of the imaginary frequency at the TS. In contrast to $\mathbf{B}_{H \text{ NCP}}$, where the movement is basically centralized at the boron, the 10-silaanthracene structure leads to a more collective motion in the molecular reorganization. As the T₁ approximation depends on only one TDA, a system

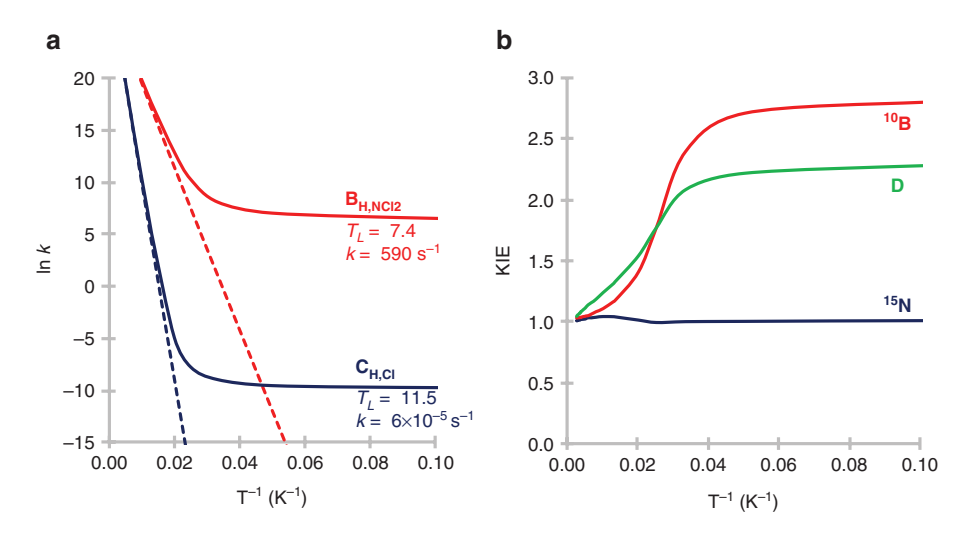


Fig. 2: (a) Arrhenius graph of the CVT (dashed lines) and CVT + SCT (curved lines) natural logarithms of the rate constants versus T^{-1} for the bell-clapper reaction of $\mathbf{B}_{H,NCI2}$ (in red) and $\mathbf{C}_{H,CI}$ (in blue) systems. (b) Kinetic isotope effects including QMT of $\mathbf{B}_{H,NCI2}$ for the boron ($^{10}B/^{11}B$), the two hydrogens connected to B (H/D) and the two nitrogens ($^{14}N/^{15}N$).

Scheme 1: 10-silaanthracene scaffold for B_{H NCI2}.

with several atoms moving concertedly interfere in the correct T_L interpretation. This acts as a warning in the use of the simple tunneling limit model.

KIE and NMR probes for tunneling

To answer the question of which atom is determining the QMT rate, we carried out several isotopic substitutions on $\mathbf{B}_{H,NCI2}$. In principle, at low temperatures where the reaction goes exclusively by tunneling, the atom with larger kinetic isotope effect (KIE) should be the "tunneling determining atom" (**TDA**), that is the one hindering the QMT process the most. However, in practice this is not so easy to define, as the mass ratio for different atomic substitutions is completely different (especially when comparing light and heavy QMT). Still, there should be a correlation between the KIEs and the atoms with the larger displacement in the imaginary normal mode of the TS (at least when comparing atoms of comparable masses). Therefore, we carried out a detailed investigation of the KIE on the atoms that showed maximum movement at the TS. A close inspection of the translation vector for $\mathbf{B}_{H,NCI2}$ system showed, as expected, a large displacement of the boron, along with a slight movement of the lateral nitrogens and the hydrogens attached to the boron.

On substitution of these atoms by their isotopic analogues, B leads to the highest KIE (10 B/ 11 B) of 2.83 at cryogenic conditions, followed by a KIE (H/D) of 2.30 for the hydrogens, while for the nitrogens is, surprisingly, negligible (1.01), as can be seen in Fig. 2b. As we said before, it is not convenient to draw a distinction between the KIEs of light and heavy atoms due to the differences in their effective masses and isotopic mass ratio. However, for our system it can be explicitly seen that among the three studied KIEs the boron atom is the TDA, reflected by its remarkably high KIE. The KIE for hydrogens is, actually, very low, considering that the D/H mass ratio (2) is enormous compared to the ratio between the boron isotopes (1.1). In addition, there are two hydrogens involved, which would make the individual KIE approximately equal to the square root of both atoms taken together (KIE ~ 1.52, considering that the hydrogens have independent influence on the KIE). We also checked the KIE (12 C/ 13 C) for the carbocation in $C_{H,CI}$, again producing a high value of 2.5, undoubtfully indicating that the reaction is occurring exclusively via QMT from the ground vibrational state, and that the carbocation is the TDA.

To provide an experimental proof for the detection of heavy atom tunneling in the bell-clapper reaction we propose the use of cryogenic solid-state NMR spectroscopy (a complicated but possible experiment [57]). The NMR coalescence temperature (T_c) is defined as the temperature at which two separate peaks of exchanging pairs of atoms merge into a single peak. At this temperature, the coalescence rate constant (k_c) is proportional to the frequency of the NMR equipment (v_{inst}) and the separation of the chemical shifts ($\Delta\delta$, in ppm), according to:

$$k_{c} = \frac{\pi}{\sqrt{2}} \Delta \delta \times v_{\text{inst}} \tag{3}$$

If the merging of peaks occurs at significantly lower temperature than what would be expected in a thermal mechanism, there we will have a sign of QMT [23, 58, 59]. Table 2 lists the computed differences in the NMR chemical shift of the exchanging pairs of atoms and the corresponding k_c values for systems $\mathbf{B}_{H,NGI2}$, $\mathbf{B}_{H,NBP2}$ and $\mathbf{C}_{H,CI}$. In all these systems the coalescence rate constants for the hydrogens and nitrogens are much smaller than Cl and Br due to its small differences in their chemical shifts.

Table 2: NMR chemical shift differences between exchanging atoms ($\Delta\delta$ in ppm, for nitrogen, chlorine, bromine, and for α , β and γ hydrogens with respect to one and eight position of the anthracene scaffold), coalescence rate constant for a 500, 50.6, 48.9, and 125.26 MHz NMR (k_c in s⁻¹) for H, N, Cl and Br, respectively, and the coalescence temperature with and without tunneling correction (T_c^{SCT} and T_c^{CVT} respectively, in K) for $\mathbf{B}_{H,NCL2}$, $\mathbf{B}_{H,NBL2}$ and $\mathbf{C}_{H,CL}$.

System	Atom	, ,	Δδ	k _c	T_c^{CVT}	T_c^{sct}
B _{H,NCl2}	Н	α	0.52	600	38	0
		β	0.08	80	34	0
		γ	0.02	25	35	0
	N		1.90	200	36	0
	Cl		243	26 500	45	40
B _{H,NBr2}	Н	α	0.49	550	46	35
		β	0.05	55	41	4
		γ	0.02	25	39	20
	N		1.09	125	42	20
	Br		786	22 000	64	60
C _{H,Cl}	Н	α	0.38	425	83	80
		β	0.16	180	80	77
		γ	0.04	45	75	72
	Cl	,	81	900	95	93

If our predictions are correct, in $\mathbf{B}_{\mathrm{H,NCI2}}$ the peaks of all the equivalent atoms except Cl should be merged at any temperature due to tunneling from the ground state; in the hypothetical absence of tunneling two peaks would be observed for hydrogens and nitrogen below ~35 K. The significant difference between T_c^{CVT} and T_c^{SCT} is a strong indication of tunneling for this system, a prediction that, although not straightforward, can be experimentally tested. For $\mathbf{B}_{\text{H.NBr2}}$ the largest difference appears at the β -hydrogen atoms, where T_{c}^{SCT} is 37 K lower than T_c^{CVT} ; only below liquid He temperature we will see two peaks, while in the absence of tunneling we would see two peaks up to 41 K. A similar but significantly less marked scenario should be seen for carbocationic system $\mathbf{C}_{\mathbf{H},\mathbf{G}}$, where such a small $T_{\mathbf{G}}$ difference with and without tunneling correction can hardly be taken as a strong proof of QMT.

Conclusions

In this paper, we have investigated intramolecular degenerate $S_N 2$ rearrangement reactions of the "bell-clapper" type, where a central boron atom (or its isoelectronic carbocation) switches bond alternatively with its lateral Lewis bases placed at one and eight position of the anthracene molecule. This rapid ping-pong like reaction can be accompanied by low activation energy and relatively narrow barrier width. Tuning of the systems by introducing relatively weak bases (such as nitrogen dihalides for the boron and halogens in the carbocation systems) at the lateral "Y" positions can significantly reduce the effective barrier width along with lowering in the energy barrier, making them an ideal system for heavy atom tunneling. Calculation including the small curvature tunneling (SCT) approximation reveals that the reaction on $\mathbf{B}_{\text{H.NCL2}}$ occurs exclusively by boron atom tunneling close to absolute zero, while the classical thermal over the barrier reaction is virtually non-existence. The remarkably high KIE for the B atom is also a witness of the QMT effect. To the best of our knowledge, this is the first example of reaction involving boron atom tunneling. Other promising candidates that are found to be driven by heavy atom tunneling are $\mathbf{B}_{\text{H.NB},2}$ and $\mathbf{C}_{\text{H.Cl}}$, where the latter involves carbon atom tunneling. Additionally, we postulate an experimental test to probe the QMT mechanism by cryogenic NMR spectroscopy.

Acknowledgements: This research was supported by the Israeli Science Foundation, Funder Id: http://dx.doi. org/10.13039/501100003977 (grant no. 631/15). A.N. acknowledges the financial support of the Negev-Tsin Scholarships.

References

- [1] R. H. Crabtree. Chem. Soc. Rev. 46, 1720 (2017).
- [2] R. J. Gillespie, B. Silvi. Coord. Chem. Rev. 233-234, 53 (2002).
- [3] J. C. Martin. Science 221, 509 (1983).
- [4] Y. Hirano, S. Kojima, Y. Yamamoto. J. Org. Chem. 76, 2123 (2011).
- [5] D. Y. Lee, J. C. Martin, J. Am. Chem. Soc. 106, 5745 (1984).
- [6] K. Akiba. Chemistry of Hypervalent Compounds, John Wiley & Sons, New York (1999).
- [7] J. I. Musher. Angew. Chem. Int. Ed. Engl. 8, 54 (1969).
- [8] W. C. McKee, J. Agarwal, H. F. Schaefer, P. von R. Schleyer. Angew. Chem. Int. Ed. Engl. 53, 7875 (2014).
- [9] M. Malischewski, K. Seppelt. Angew. Chem. Int. Ed. 56, 368 (2017).
- [10] J. Jašík, D. Gerlich, J. Roithová. J. Am. Chem. Soc. 136, 2960 (2014).
- [11] A. Karim, N. Schulz, H. Andersson, B. Nekoueishahraki, A.-C. C. Carlsson, D. Sarabi, A. Valkonen, K. Rissanen, J. Gräfenstein, S. Keller, M. Erdélyi. J. Am. Chem. Soc. 140, 17571 (2018).
- [12] G. P. McGovern, D. Zhu, A. J. A. Aquino, D. Vidović, M. Findlater. Inorg. Chem. 52, 13865 (2013).
- [13] C. Dou, S. Saito, S. Yamaguchi. J. Am. Chem. Soc. 135, 9346 (2013).
- [14] M. R. Siebert, D. J. Tantillo. J. Org. Chem. 71, 645 (2006).
- [15] V. V. Zhdankin. in Advances in Heterocyclic Chemistry, E. F. V. Scriven, C. A. Ramsden (Eds.), vol. 119, pp. 57-79, Academic Press, New York, USA (2016).
- [16] R. M. Minyaev, T. N. Gribanova, V. I. Minkin. in Comprehensive Inorganic Chemistry II (Second Edition), J. Reedijk, K. Poeppelmeier (Eds.), pp. 109-132, Elsevier, Amsterdam (2013).
- [17] S. C. A. H. Pierrefixe, S. J. M. van Stralen, J. N. P. van Stralen, C. Fonseca Guerra, F. M. Bickelhaupt. Angew. Chem. Int. Ed. 48, 6469 (2009).
- [18] I. Fernández, E. Uggerud, G. Frenking. Chem. Eur. J. 13, 8620 (2007).
- [19] K. Akiba, Y. Moriyama, M. Mizozoe, H. Inohara, T. Nishii, Y. Yamamoto, M. Minoura, D. Hashizume, F. Iwasaki, N. Takagi, K. Ishimura, S. Nagase. J. Am. Chem. Soc. 127, 5893 (2005).
- [20] M. Yamashita, Y. Yamamoto, K. Akiba, D. Hashizume, F. Iwasaki, N. Takagi, S. Nagase. J. Am. Chem. Soc. 127, 4354 (2005).
- [21] T. R. Forbus, J. C. Martin. J. Am. Chem. Soc. 101, 5057 (1979).
- [22] T. R. Forbus, J. C. Martin. Heteroatom Chem. 4, 113 (1993).
- [23] A. Nandi, A. Sucher, S. Kozuch. Chem. Eur. J. 24, 16348 (2018).
- [24] R. P. Bell. The Tunnel Effect in Chemistry, Chapman & Hall, London; New York (1980).
- [25] R. K. Allemann, N. S. Scrutton. Quantum Tunnelling in Enzyme-catalysed Reactions, RSC, Cambridge (2009).
- [26] W. T. Borden. WIREs Comput. Mol. Sci. 6, 20 (2016).
- [27] D. W. Whitman, B. K. Carpenter. J. Am. Chem. Soc. 102, 4272 (1980).
- [28] D. W. Whitman, B. K. Carpenter. J. Am. Chem. Soc. 104, 6473 (1982).
- [29] B. K. Carpenter. J. Am. Chem. Soc. 105, 1700 (1983).
- [30] P. S. Zuev, R. S. Sheridan, T. V. Albu, D. G. Truhlar, D. A. Hrovat, W. T. Borden. Science 299, 867 (2003).
- [31] A. Datta, D. A. Hrovat, W. T. Borden. J. Am. Chem. Soc. 130, 6684 (2008).
- [32] O. M. Gonzalez-James, X. Zhang, A. Datta, D. A. Hrovat, W. T. Borden, D. A. Singleton. J. Am. Chem. Soc. 132, 12548 (2010).
- [33] X. Zhang, D. A. Hrovat, W. T. Borden. Org. Lett. 12, 2798 (2010).
- [34] T. Schleif, J. Mieres-Perez, S. Henkel, M. Ertelt, W. T. Borden, W. Sander. Angew. Chem. Int. Ed. 56, 10746 (2017).
- [35] H. Inui, K. Sawada, S. Oishi, K. Ushida, R. J. McMahon. J. Am. Chem. Soc. 135, 10246 (2013).
- [36] S. L. Buchwalter, G. L. Closs. J. Am. Chem. Soc. 97, 3857 (1975).
- [37] S. L. Buchwalter, G. L. Closs. J. Am. Chem. Soc. 101, 4688 (1979).
- [38] C. Doubleday, R. Armas, D. Walker, C. V. Cosgriff, E. M. Greer. Angew. Chem. Int. Ed. 56, 13099 (2017).
- [39] J. Meisner, J. Kästner. Angew. Chem. Int. Ed. 55, 5400 (2016).
- [40] T. K. Mandal, S. K. Pati, A, Dutta. J. Phys. Chem. A. 113, 8147 (2009).
- [41] J. O. Richardson. Phys. Chem. Chem. Phys. 19, 966 (2017).
- [42] C. Qu, J. M. Bowman, Phys. Chem. Chem. Phys. 18, 24835 (2016).
- [43] H. S. Yu, X. He, S. L. Li, D. G. Truhlar. Chem. Sci. 7, 5032 (2016).
- [44] M. J. Frisch, G. W. Trucks, H. B. Schlegel, G. E. Scuseria, M. A. Robb, J. R. Cheeseman, G. Scalmani, V. Barone, G. A. Petersson, H. Nakatsuji, X. Li, M. Caricato, A. V. Marenich, J. Bloino, B. G. Janesko, R. Gomperts, B. Mennucci, H. P. Hratchian, J. V. Ortiz, A. F. Izmaylov, J. L. Sonnenberg, D. Williams-Young, F. Ding, F. Lipparini, F. Egidi, J. Goings, B. Peng, A. Petrone, T. Henderson, D. Ranasinghe, V. G. Zakrzewski, J. Gao, N. Rega, G. Zheng, W. Liang, M. Hada, M. Ehara, K. Toyota, R. Fukuda, J. Hasegawa, M. Ishida, T. Nakajima, Y. Honda, O. Kitao, H. Nakai, T. Vreven, K. Throssell, J. A. Montgomery, Jr., J. E. Peralta, F. Ogliaro, M. J. Bearpark, J. J. Heyd, E. N. Brothers, K. N. Kudin, V. N. Staroverov, T. A. Keith, R. Kobayashi, J. Normand, K. Raghavachari, A. P. Rendell, J. C. Burant, S. S. Iyengar, J. Tomasi, M. Cossi, J. M. Millam, M. Klene, C. Adamo, R. Cammi, J. W. Ochterski, R. L. Martin, K. Morokuma, O. Farkas, J. B. Foresman, D. J. Fox. Gaussian 16, Revision A.03, Gaussian, Inc., Wallingford, CT (2016).

- [45] D. G. Liakos, F. Neese. J. Chem. Theory Comput. 11, 4054 (2015).
- [46] C. Riplinger, F. Neese. J. Chem. Phys. 138, 034106 (2013).
- [47] F. Neese. WIREs Comput. Mol. Sci. 2, 73 (2012).
- [48] D. G. Liakos, M. Sparta, M. K. Kesharwani, J. M. L. Martin, F. Neese. J. Chem. Theory Comput. 11, 1525 (2015).
- [49] A. Fernandez-Ramos, B. A. Ellingson, B. C. Garrett, D. G. Truhlar. in *Reviews in Computational Chemistry*, K. B. Lipkowitz, T. R. Cundari (eds.), pp. 125–232. Wiley-Blackwell, Hoboken (2007).
- [50] W.-P. Hu, Y.-P. Liu, D. G. Truhlar. J. Chem. Soc. Faraday Trans. 90, 1715 (1994).
- [51] D. G. Truhlar, B. C. Garrett. Annu. Rev. Phys. Chem. 35, 159 (1984).
- [52] J. Zheng, J. L. Bao, R. Meana-Pañeda, S. Zhang, B. J. Lynch, J. C. Corchado, Y.-Y. Chuang, P. L. Fast, W.-P. Hu, Y.-P. Liu, G. C. Lynch, K. A. Nguyen, C. F. Jackels, A. Fernandez Ramos, B. A. Ellingson, V. S. Melissas, J. Villà, I. Rossi, E. L. Coitiño, J. Pu, T. V. Albu, A. Ratkiewicz, R. Steckler, B. C. Garrett, A. D. Isaacson, D. G. Truhlar. *POLYRATE version 2017*, University of Minnesota, Minneapolis (2017).
- [53] J. Zheng, J. L. Bao, S. Zhang, J. C. Corchado, R. Meana-Pañeda, Y.-Y. Chuang, E. L. Coitiño, B. A. Ellingson, D. G. Truhlar. GAUSSRATE 17-B, University of Minnesota, Minneapolis, MN (2017).
- [54] J. G. Lauderdale, D. G. Truhlar. Surf. Sci. 164, 558 (1985).
- [55] S. Kozuch. Phys. Chem. Chem. Phys. 16, 7718 (2014).
- [56] J. C. Martin, R. J. Basalay. J. Am. Chem. Soc. 95, 2572 (1973).
- [57] C. S. Yannoni, V. Macho, P. C. Myhre, J. Am. Chem. Soc. 104, 7380 (1982)
- [58] H. Friebolin. Basic One- and Two-Dimensional NMR Spectroscopy, Wiley-VCH, Weinheim (2011).
- [59] E. Solel, S. Kozuch. J. Org. Chem. 83, 10826 (2018).